5 February 1982, Volume 215, Number 4533 SCIENCE

Positron Tomography and Nuclear Magnetic Resonance Imaging

Gordon L. Brownell, Thomas F. Budinger
Paul C. Lauterbur, Patrick L. McGeer

Summary. Noninvasive imaging methods for medical diagnosis and biological investigations have evolved from qualitative radiological techniques to quantitative methods of measuring biochemical and physiological processes in the human body. In particular, new developments in emission tomography, nuclear magnetic resonance imaging, and in vivo spectroscopy offer new horizons for medical research and clinical activities. These methods and their potentials are reviewed and contrasted.

In the past 10 years new approaches and notable advances in medical imaging have resulted from new concepts and developments in computer science and applied mathematics. A major emphasis in diagnostic instrument development has been on the three-dimensional description of physiological and biochemical processes in health and disease. Six modalities that have evolved or have been markedly improved, along with the major biological and physical parameters measured by these methods, are shown in Table 1.

The underlying principles of new methodologies and their status and potential were examined at a recent conference (*1*). The emphasis of the conference, however, was largely on positron emission tomography (PET) and nuclear magnetic resonance (NMR) because these methods convey information about body chemistry and physiology, normal and abnormal. There was less emphasis on methods that provide improvements in imaging anatomy (computed tomography and heavy-ion imaging) or the motion and location of surfaces and blood vessels (transmission computed tomography and ultrasound imaging). The coverage was in no way meant to indicate an assessment of the ultimate usefulness of each modality; for example, although digital subtraction radiography is of widespread interest and demonstrated efficacy, it was not covered at the conference.

The potentials and to some extent the medical applications of each modality can be appreciated from an examination of Table 1, which emphasizes that it is the parameter measured, rather than image resolution or display quality, that is important for selection of an imaging technique in a particular disease condition. Schizophrenia is now believed by many to be a metabolic disease without consistent evidence for structural abnormalities. Thus to investigate this condition one would select a technique that measures biochemical function rather than anatomy. Positron tomography appears to offer great potential for the study of possible chemical defects. Although NMR is not sufficiently sensitive for high-resolution imaging of the distribution of elements other than hydrogen, it can measure the relative concentration of adenosine triphosphate (ATP) and creatine phosphate in selected regions of the brain. Thus, both PET and NMR have specific yet different roles in the study of this and other mental diseases.

By contrast, tomography is not required for the measurement of the amount of blood ejected by each heart contraction. In practice, blood is labeled with a suitable radiopharmaceutical to observe the image of the left ventricular blood pool before and after heart contraction (*2*). Because labeled blood in the heart ventricles is detected without serious interference from background activity, the nuclear medicine procedure of cineangiography can give the desired information without the need for tomographic methods. Of course, x-ray computed tomography (CT) with contrast material (*3*) or digital subtraction methods with x-rays (*4*) can be used, but the radionuclide procedures are at present less invasive and appear to be more efficacious.

Emission Tomography

There are important physical and biological differences between x-ray transmission tomography and emission tomography. The basic physical difference is that in emission tomography the information sought is the source and intensity of the gamma radiation emitted by the isotope; in x-ray transmission tomography the distribution of the tissue densities or attenuation coefficients is sought. A consequence of this difference is the need in emission tomography to compensate for the effect of attenuation. This is achieved by incorporation of the attenuation coefficients in the image reconstruction methods (*5*). Emission tomography measures regional function (Table 1), whereas x-ray CT describes regional structure or anatomy.

The earliest clinical use of emission

Gordon L. Brownell is a professor at Massachusetts Institute of Technology and director, Physics Research Laboratory, Massachusetts General Hospital, Boston 02114; Thomas F. Budinger is Henry Miller professor of medical research, Donner Laboratory and Department of Electrical Engineering and Computer Sciences, University of California, Berkeley 94720; Paul C. Lauterbur is a professor in the Department of Chemistry and research professor in the Department of Radiology, State University of New York, Stony Brook 11794; and Patrick L. McGeer is a professor in the Department of Neurosciences, University of British Columbia, Vancouver, British Columbia, Canada V6T 1W5. For reprints contact T. F. Budinger.

0036-8075/82/0205-0619$01.00/0

transverse section tomography was the work of Kuhl and Edwards (*6*) in the early 1960's. Later, the emission longitudinal tomographic scanner for limited angle tomography was developed by Anger (*7*). Single-photon tomography preceded x-ray CT and provided the first demonstration of quantitative physiological studies (*8*). Recently, through new developments, single-photon tomography has been shown to be a practical clinical tool for the measurement of cerebral blood volume and regional cerebral blood flow (*9*).

Approximately 30 years ago (*10*) it was recognized that the position of a positron-emitting radionuclide could be determined because the two photons produced upon the annihilation of the positive electron (positron) with a negative electron are emitted 180° from one another. Thus by positioning detectors around a patient it is possible to determine the line along which a disintegration occurred (Fig. 1a). The availability of physiologically interesting positron-emitting radiopharmaceuticals and of suitable instrumentation, as well as the development of algorithms for computed tomographic image reconstruction, provided the impetus for PET (*5, 11*).

An advantage of PET over single-photon tomography is its much greater efficiency or sensitivity for detecting radiopharmaceuticals, because in the single-photon technique physical collimation results in loss of many available photons. The ability to label compounds with positron-emitting isotopes of carbon, nitrogen, oxygen, and fluorine is the basis for great expectations from PET. To produce radiopharmaceuticals containing these radionuclides it is necessary to have available a cyclotron or, for some positron emitters, a portable generator. By contrast, single-photon emitters, for instance, ^{99m}Tc and ^{123}I, can be obtained from noncyclotron or remote sources, and they are easier to work with because of their longer half-lives.

Instrumentation for Positron Emission Tomography

Recent reviews of positron imaging and tomographic instrumentation are cited in (*12–14*). The first positron imaging system was developed at Massachusetts General Hospital in 1953; it was followed by a series of positron cameras including the tomographic positron camera PC-II (*15*), the PETT scanner at Washington University (*16, 17*), and other PET instruments at Brookhaven National Laboratory, Montreal Neurological Institute (*18*), Donner Laboratory at the University of California, Berkeley (*14, 19*), and other centers (*20*). Commercial systems are now available from four sources (the Cyclotron Corporation, California; ORTEC, Tennessee; Atomic Energy of Canada; and Scandatronics, Sweden). All commercial systems have approximately the same characteristics. They have rings of bismuth germanate ($Bi_4Ge_3O_{12}$) detectors individually coupled or coded to photomultiplier tubes. Employment of cross coincidences between rings results in more image levels than the number of individual rings of crystals; thus a four-ring system can give data for seven planes.

The sensitivity of these systems is usually given in terms of the number of events per second for a phantom 20 centimeters in diameter uniformly filled with a water solution containing 1 microcurie of a positron emitter per cubic centimeter; it is denoted here by S^{-1}. This unit is convenient for expressing sensitivity, particularly for brain imaging devices. Sensitivity ranges from 1×10^4 to 5×10^4 S^{-1} per plane, and the sensitivity of multilayer systems comprising two or more adjacent rings of crystals is greater. Thus four-ring systems have sensitivities of 1×10^5 to 5×10^5 S^{-1}. It has been suggested (*13*) that the unit be defined for a 20-cm-diameter sphere since the sensitivity per plane is virtually identical to that of a 20-cm-diameter cylinder even for a multiplanar system. This source has a finite upper limit of 3.25×10^7 S^{-1} for the number of detectable transformations per unit time. Thus the most powerful devices now available have sensitivities 100 times less than the theoretical maximum.

Recent trends in positron instrumentation have been in two directions. The first is toward high-resolution positron instruments (*14, 19, 20*); the second is toward the use of time of flight to improve image quality (*21*). High resolution is achieved by using many thin detectors in a ring configuration. Since photoelectron tubes have relatively large dimensions, various coding schemes have been proposed to identify individual detectors, and this aspect of the design may become limiting unless a new phototube is developed. Alternatively, clever coding schemes (*13*) can identify 420 detectors with 84 photoelectron tubes in one ring.

Many factors limit the ultimate resolution of positron imaging systems. The most important are the distance the positron travels through tissue before annihilation, the angular deviation of ±0.25° from 180° for the two photons emitted on annihilation, finite detector dimensions, and statistical aspects of reconstruction. Depending on the isotopes and the ring dimensions, the first two factors set a limit of a few millimeters on the resolution defined as full width at half-maximum (FWHM), which is the smallest separation at which two signal sources can be placed and still be detected. Practical considerations in the construction of the detectors, problems in mechanical coupling to photoelectron tubes, and the physical limitations of supporting the crystal array limit the detector width. Improvement in scintillation detectors (*22*) involves the development of a detector with the high efficiency of bismuth germanate, the speed of CsF, and the light output of NaI(Tl). Fast detectors are needed to facilitate separation of true

Table 1. Comparison of medical imaging techniques.

Method	Parameters measured	Medical applications
Transmission computed tomography	Density and average atomic number	Anatomy, mineral content, movement of contrast material
Emission computed tomography (positron and single photon)	Concentrations of radionuclides	Metabolism, receptor site concentration, flow
Nuclear magnetic resonance (imaging or in vivo spectroscopy)	Concentration of nuclides such as ^1H, relaxation parameters T_1 and T_2, frequency shifts due to chemical form	Free water content, relative flow, concentrations of some molecular species and contrast agents
Digital subtraction radiography	Contrast distribution	Flow channel anatomy (angiography)
Ultrasound	Acoustic impedance mismatches, sound velocity, attenuation, frequency shifts due to motion	Anatomy, tissue structural characteristics, flow
Heavy ion radiography	Density (electron)	Anatomy (high resolution)

coincident events from false coincidences, which occur at high data rates. However, the statistical uncertainty in reconstruction resulting from the finite number of detected events is the principal factor limiting the resolution of positron tomographs (*23*). Most current instruments produce images with a resolution of 10 to 20 mm FWHM. Resolutions of 6 to 7 mm are claimed for proposed instruments, but these systems have not yet been completed. It is unlikely that instruments with resolutions less than 4 mm will be available in the foreseeable future.

It is hoped that time-of-flight instrumentation will improve image quality. The aim is to limit the uncertainty along the track from which the annihilation event occurred by detecting the time difference in arrival of the photons at the opposed detectors (Fig. 1b). The improvement in statistics of the reconstructed image is in the ratio of the 1/2 power of the diameter of the object to the resolution in distance of the position along the track as determined by time of flight. This is currently approximately 500 picoseconds or 7.5 cm with cesium fluoride crystals. Imaging devices in which this concept is used are being constructed (*21*).

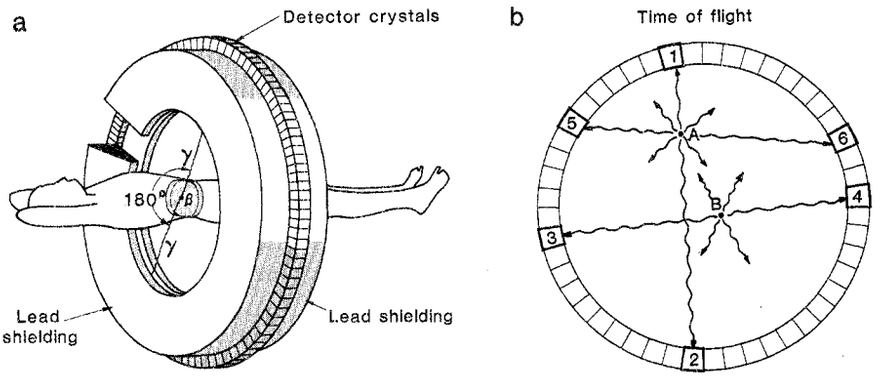

Fig. 1. Positron emission tomography. Positron-emitting radiopharmaceuticals such as ^{15}O or ^{11}C emit a positive electron, which, after traveling a few millimeters from the nucleus, interacts with a negative electron. The resulting annihilation yields two 511-kiloelectron volt photons, which fly off at 180° from one another. Typically, after an intravenous injection of a low dose of the radiopharmaceutical, 1 million of these photons are detected in time coincidence by scintillation crystals mounted in one or more rings surrounding the patient (a). Most PET imaging devices use time coincidence to determine the line of position along which the positron emitter decayed. In addition, the small differential in time of arrival of the annihilation photons can be used to estimate the position of the source along this line of flight (b). A time difference in arrival at two detectors of 300 picoseconds corresponds to a 9-cm travel difference at the speed of light or a position resolution of 4.5 cm FWHM. This time-of-flight concept is proposed for future instruments (*21*).

Radiopharmaceutical Development

Cyclotron production of radionuclides and preparation of useful positron emitters have been reviewed (*24*). Radiopharmaceuticals are being developed for (i) substrate labeling, (ii) substrate analog labeling, (iii) labeling of drugs involved in normal or pathological biochemical pathways (for instance, sugars, fatty acids, and amino acids), (iv) labeling of ligands for receptor binding sites, and (v) labeling of proteins, antibodies, cells, or particles.

In the first category, ^{11}C-labeled glucose (*25*), ^{15}O-labeled water, and $^{15}O_2$ itself have been used to trace these important substrates (*26, 27*). Amino acids have been labeled with ^{13}N (*28*). The best known labeled analog is ^{18}F-labeled 2-deoxyglucose (*29*), which has been widely used in studies of the brain. Labeling of drugs for studies of the brain (*30*) and other organs is an important area of research. The labeling of ligand agonists or antagonists for receptor binding, such as spiroperidol (*31*) or flunitrazepam (*32*), has also been studied. Finally, labeled antibodies should have wide application in studies of many organs if the specificity of the antibodies is sufficiently great.

Because of the short half-lives of the radionuclides, new synthetic procedures are usually required. Thus the development and evaluation of a new radiopharmaceutical usually requires more than 2 years, with close collaboration between chemists, physicists, physiologists, and physicians.

Kinetic Analysis in vivo

Computed tomography with positron-emitting isotopes can determine moment-to-moment changes in tissue nuclide concentrations in situations where the statistics are adequate (*23*). Modeling techniques employed in classical physiology must be used along with the information from PET. Many models require dynamic information, but due to limited statistics moment-to-moment information cannot often be obtained. Moreover, the tomographic method cannot distinguish the labeled metabolite from labeled metabolic products. This has encouraged the search for analogs of natural metabolites. The ideal analog would behave exactly like the substrate up to a certain point in the metabolic process, but would then be trapped. Sugar and fatty acid analogs that approach this goal have been developed. The interpretation of data obtained with analogs is embodied in biological modeling; because of their ease of analysis, compartmental models have usually been used.

One of the most important physiological quantities common to all tissues of the body is blood flow. It is most directly measured by introducing into the bloodstream a bolus of labeled water or other diffusible tracers labeled with positron-emitting radionuclides and following them by dynamic imaging. From the washout curve and appropriate partition coefficients, tissue blood flow may be determined accurately. Sequential images are required to use this method with positron emitters such as ^{77}Kr (*33*) and procedures similar to those employed with ^{133}Xe and single-photon emission tomography (*9*).

A second procedure for determining blood flow involves equilibrium imaging (*27, 34*). Labeled water is produced in the lungs by continuous inhalation of $C^{15}O_2$. After several half-lives (4 to 6 minutes for ^{15}O) a steady-state distribution is observed. In effect, the steady-state condition is reached when the disappearance due to the physical half-life is balanced by the flow-dependent accumulation. Blood flow can be determined from the images by use of a simple mathematical model. The advantage of a stationary distribution is that higher resolution images can be produced; however, the relation between cerebral blood flow and activity is nonlinear and the accuracy is limited at high flow.

A third technique involves injection of radiopharmaceuticals that are extracted in proportion to blood flow and, once extracted, remain trapped in the tissues. This is analogous to the use of radiolabeled microspheres 9 to 15 micrometers in diameter; however, except for lung imaging, injection of degradable microspheres is not feasible. The agents that

are most commonly used and have good extraction in the heart and kidneys are $^{13}NH_3$ (*35*) and ^{82}Rb (*36*). Agents for brain studies have been developed for single-photon tomography (*9*), but are still under development for positron tomography.

Oxygen utilization (*37*) may also be determined by the equilibrium method with $^{15}O_2$. Although principally used in the brain, the method may be used for other tissues, particularly for tumor studies.

Most models involve assumptions because one or more of the following factors are unknown: exact concentration delivered to the tissue, local blood flow, cell mass available to the radiopharmaceutical, chemical form of the label, permeability changes accompanying the disease state, and specificity of the tracer. Nevertheless, remarkably precise regional physiological data have been obtained with positron tomography. Values for blood flow and glucose metabolism with accuracies of 10 to 20 percent have been reported, and a relative precision of 5 percent or less is common. Considering that the object may have thousands of volume elements, the amount of information obtained is great.

Medical Science Applications

Knowledge of blood flow in the brain is important in the evaluation of stroke and other diseases. Equilibrium imaging of $H_2{}^{15}O$ (*27, 34, 37, 38*) and $^{13}NH_3$ extraction have been used for this purpose. Blood volume may be determined by use of intravascular tracers such as ^{11}CO-labeled red cells (*39*). Single-photon tomography can compete with positron tomography for these measurements at low resolution (*9*).

Since the brain uses glucose as a primary energy source, labeled forms of glucose should be useful for mapping the brain's energy consumption (*40*). The method has the advantage of relatively few assumptions, but it suffers from the poor resolution common to most dynamic measurements due to their limited statistics. Sokoloff (*41*) developed the ^{14}C-labeled deoxyglucose technique for autoradiographic mapping of glucose metabolism in animal brain. Reivich *et al.* (*42*) subsequently showed that ^{18}F-labeled deoxyglucose (FDG) could be used in a similar manner for PET in vivo imaging. This technique has been refined and applied by a number of groups (*43*).

Glucose metabolism followed with FDG appeared to be a more sensitive indicator of brain damage and recovery than tissue perfusion observed by $^{13}NH_3$ (*44*). Similarly, oxygen metabolism seems to be a more consistent and reliable index of tissue injury than cerebral blood flow (*45*). The combination of perfusion metabolism and permeability data (*46*) can give important information on disease processes.

A particularly fascinating possibility for PET is the delineation of neural pathways that respond to sensory stimulation. Perhaps the clearest demonstration of this effect has been through stimulation of the visual cortex and subsequent observation of increased glucose metabolism and blood flow (*47*). This phenomenon was observed in animals with ^{14}C-labeled deoxyglucose and autoradiography (*48*), and, with another autoradiographic technique (*49*), a banding phenomenon in the visual cortex was discovered from dominance columns having a spacing of about 400 μm. Although such structures will not be seen by PET, the extensive detail seen by postmortem autoradiographic examination of animal brain is a strong impetus to improve resolution in human tomography.

Studies of the heart have paralleled those of the brain. Perfusion measurements have been made with $^{13}NH_3$ (*35*) or ^{82}Rb (*36*), and metabolism measurements with FDG and ^{11}C-labeled palmitic acid. Palmitic acid has been used to evaluate the presence of infarcts as well as regional rates of beta-oxidation (*50*), and FDG has been used to investigate glycolytic rates (*51*). The heart is particularly difficult to image as it is in motion and lies within a greater attenuating medium than the brain.

Techniques for gating the heart have been developed to obtain sequences of positron tomograms that reveal changes in the blood pool (*52*) and to allow extraction of the time rate of change of the arterial concentration. The agent most often used is ^{11}CO-labeled hemoglobin. Although ^{18}F concentrates in artificially induced infarcts in dog hearts (*53*), efforts to apply the technique to man have not been as successful as single-photon techniques with ^{99m}Tc-labeled pyrophosphates (*54*). Infarct imaging and quantitation remains a fertile yet underdeveloped area of positron tomography.

Techniques similar to those outlined for brain and heart can be used to study the pathophysiology of other organs and disease states and possibly to evaluate methods of therapy (*55*). Investigations of cancer and vascular disease have employed measurements of blood flow by $C^{15}O_2$ equilibrium imaging methods and of metabolism with FDG.

Future of Positron Emission Tomography

The PET technique has the potential for measurement of sugar, fatty acid, amino acid, and other substrate metabolism as well as receptor concentration anywhere in the body. Thus there is no question that it is a valuable new research tool for the investigation of life processes in such difficult to study diseases as aging, schizophrenia, atherosclerosis, and cancer. Although work is proceeding on instrumentation, radiopharmaceuticals, and modeling, the real need is for biological information as a prelude to clinical utility. Associated with emission tomography are small risks from ionizing radiation similar to those in other diagnostic procedures. The benefits should far outweigh these risks.

Nuclear Magnetic Resonance Imaging

The use of NMR to study living tissues began in 1968 with quantitative hydrogen NMR measurements on excised but functional frog muscles and, within a few years, on water and fat in the arms of living humans and in the living rat (*56*). Since differences in the NMR properties of normal and malignant rat tissue were reported in 1971 (*57*) and NMR was used to form images in 1972 (*58*), activity has focused on the perfection of noninvasive NMR measurements of the human body. Observations in 1973 (*59*) of the relation between phosphorus NMR spectra and metabolites of red blood cells heralded the in vivo evaluation of concentrations of high-energy phosphate compounds such as ATP and creatine phosphate.

The theory of NMR is discussed in (*60*). Most elements have at least one reasonably abundant isotope whose nucleus is magnetic. In an external magnetic field such a nucleus (which can be thought of as a small magnet) can assume a low-energy state when aligned with the field or a higher energy state when aligned against the field. A weak but rapidly alternating magnetic field applied by a coil near the subject or specimen stimulates changes in the orientation of the nucleus relative to the direction of a strong static magnetic field (Figs. 2 and 3). This results in absorption of energy, which is emitted when the nucleus returns to the equilibrium state. The absorption and emission of energy take place at the resonance frequency, given by the formula $\nu = \gamma H/2\pi$, where γ is the characteristic gyromagnetic ratio and H is the static magnetic field. The nuclei

of different elements, and even of different isotopes of the same element, have very different frequencies. For a field of 0.1 tesla (1000 gauss) the resonance frequency of hydrogen is 4 megahertz and that of phosphorus is 1.7 MHz. Electrons in the molecule containing the nucleus cause small differences in the resonance frequencies. NMR spectroscopy identifies these frequencies and gives information on molecular identity and structure.

Spatial distribution information can be obtained by using the fact that the resonance frequency depends on the magnetic field. By varying the field in a known manner through the specimen volume it is possible to select the region of the specimen from which the information is derived based on the frequency of the signal. The strength of the signal at each frequency can be interpreted as the density of the hydrogen nuclei in the plane within the object where the magnetic field corresponds to that frequency (Fig. 4).

Thus nuclei in the entire volume within or near the loops or coils of wire act as radio-frequency (RF) receiving and transmitting antennas. The transmitted signals from the nuclei are converted by various techniques into spectra, images, or both. The signals contain quantitative information on the overall concentration of the nuclei and the numbers of nuclei of a single species in different molecular environments.

The time variation of the NMR signal gives two other parameters of biological importance: the spin-lattice relaxation time T_1 and the spin-spin relaxation time T_2. These parameters depend on the motions of the nuclei, the regional temperature, the viscosity of the tissue, and the magnetic effects of nearby nuclei. The relaxation times of hydrogen nuclei in tissue give information about the local tissue conditions and are believed to carry information about disease states of the tissue. Relaxation times can be measured at each point of an image. Hydrogen signals from tissue water have different relaxation times in different organs and, although T_1 and T_2 increase in proportion to water content, there is a departure from a strict relation between relaxation times and water content in various disease states, because not all tissue constituents are equally effective in reducing the relaxation times. Natural T_1 differences (*61*) can be selectively altered or increased by the injection of paramagnetic substances such as Mn^{2+} (*62*). This is analogous to the use of x-ray contrast agents or radioactive tracers to follow flow or permeability. Flow is another parameter available from the NMR signal. It was investigated in the nonimaging mode more than 20 years ago and has a potential for use in spatial distribution studies with contemporary imaging techniques (*63–65*).

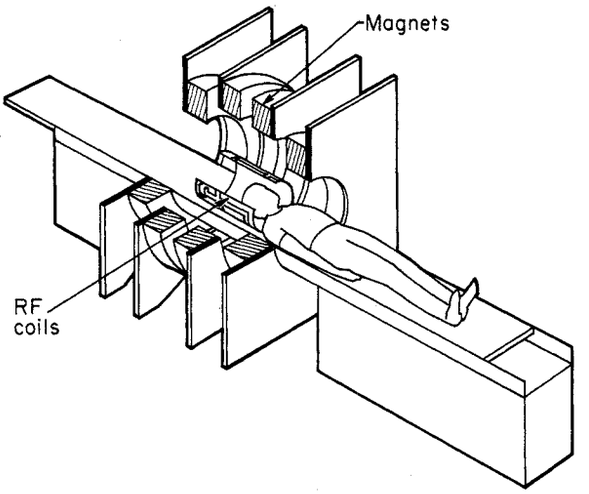

Fig. 2. Typical arrangement of solenoid coils for whole body imaging with a resistive magnet. Within the main magnet is shown the RF coil surrounding the body part to be imaged.

The medical application of NMR that is closest to existing diagnostic methods is the production of cross-sectional images similar to those generated by x-ray CT. In the case of NMR the images reflect the distribution of hydrogen and of T_1 and T_2. In patient studies with NMR the outlines of organs, structures, and lesions can be displayed at a resolution of about 2 mm FWHM at present. For small specimens, better resolution is obtained. Of even greater interest is the fact that differences in relaxation times between soft tissues such as fat, muscle, and blood are much greater than hydrogen concentration differences. Because the NMR signals received convey information dependent on the time duration of RF pulses in the stimulating coil and the time interval between pulses as well as the method of data analysis, particular NMR images depend on the instrument setting; thus some confusion can arise about the interpretation of early images (*62*) and the potential of the NMR technique in general. Most NMR images re-

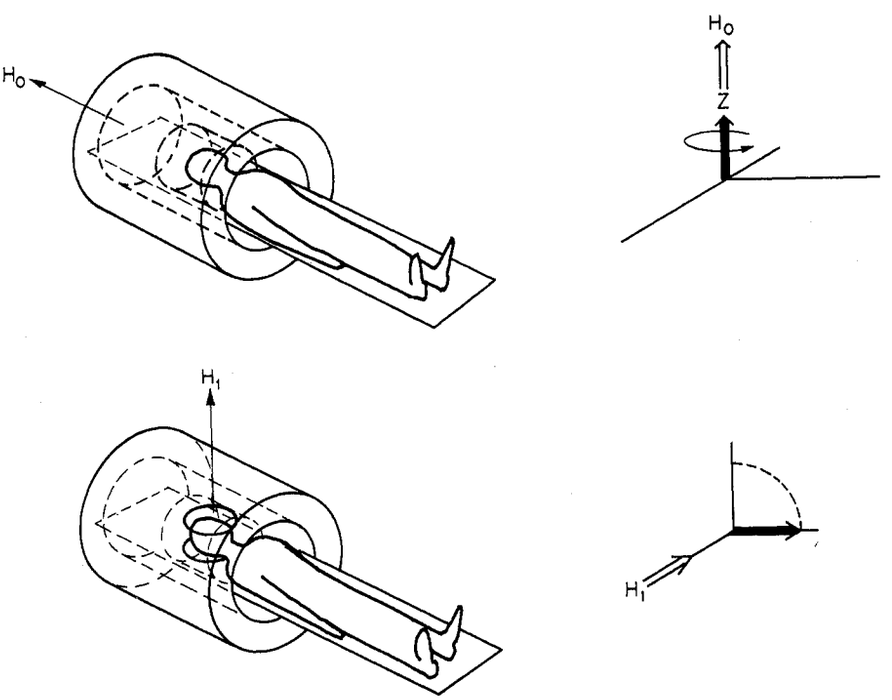

Fig. 3. Schematic of the NMR method. A static field H_0 is used to align spinning nuclei with magnetic moments. A relatively weak RF magnetic field H_1, generated from the RF coils surrounding the patient, perturbs the aligned nuclei. A voltage is generated by the interaction of the magnetic field from these nuclei with the coil. The strength and time dependence convey information about the concentration and chemical environment of these nuclei.

flect some complex combination of proton concentration, T_1, and T_2, but these three parameters can be separated into almost pure images (*61, 66*).

There are many different methods of obtaining spatial information in NMR imaging. The frequency of the received signal can be related to the preestablished magnetic field gradient over the specimen (Fig. 4). Another method involves oscillating the magnetic field gradient in different directions while leaving a line or point at a known position unperturbed, and then moving this line or point back and forth to generate an image (*67*). Alternatively, the selected volume can be fixed and the object moved through it (*68*). An increase in efficiency of spatial imaging can be obtained by recording signals simultaneously from an entire plane, then using Fourier transforms and other data processing methods for deducing a cross-sectional image similar to those produced by x-ray CT. Application of mathematical properties of the Radon transform have led to a direct and efficient procedure for reconstruction of a true three-dimensional image (*69*). However, the total time required to obtain good spatial resolution will be of the order of a few minutes, so that motion is an important problem and limitation for NMR. One of the powers of the NMR technique is the fact that by electronic changes in the instrument, planes or sections through the patient other than transaxial can be obtained without reconstitution of multiple transverse sections, as demonstrated by the University of Nottingham group (*64, 70*).

The potentials of NMR should not be compared directly with those of PET for research or clinical work, as these two techniques measure quite different parameters; PET measures distribution volumes, chemistry, and kinetics with high sensitivity, while NMR measures mainly the concentration and state of hydrogen nuclei in matter with high resolution. On the other hand, it is appropriate to make some comparison between proton NMR imaging and x-ray CT. Information on the density and state of hydrogen nuclei in tissues can convey anatomic information regarding the location and edges of organs and pathophysiological processes, just as can density and attenuation coefficient information from x-ray CT.

At present, NMR systems can achieve a resolution similar to that of x-ray CT. Although NMR measurements of the concentration of hydrogen nuclei might not depict changes between gray and white matter, or even blood and muscle, to any great extent, T_1 images give a greater contrast sensitivity than achieved by x-ray CT. It is possible to differentiate between these tissue types and lesions (*71*) with an almost twofold difference in the T_1 parameter in situations where x-ray attenuation coefficients differ by only a few percent. Thus it appears at present that competition does exist between NMR and x-ray CT for detection of the anatomic distributions related to pathophysiological processes.

The resolution and contrast sensitivity capabilities of NMR are dependent on the size of the object being imaged because both noise and the potential for distortions increase with the size of the subject immersed in the NMR coils. The resolution in NMR images is ultimately limited by the ability to detect voltages induced in the receiver coil by the nuclei. The limit is reached when the signals from the decreasing volume being observed are obscured by the noise generated within the object and the apparatus.

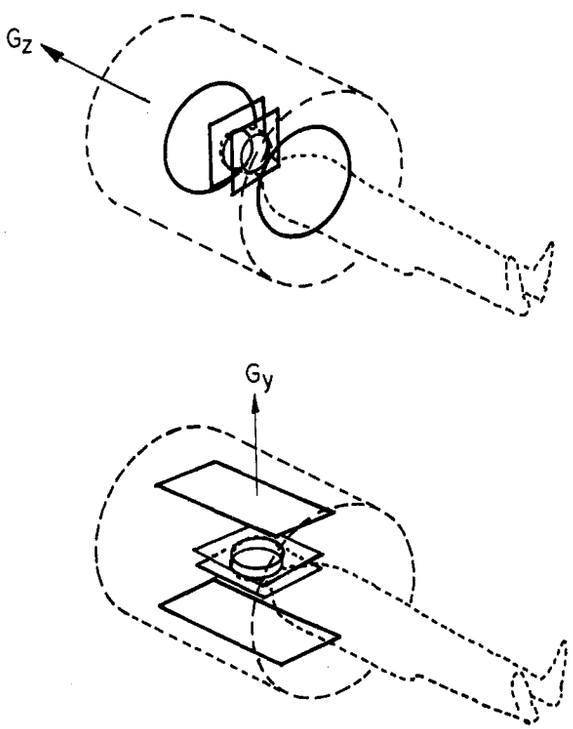

Fig. 4. Use of NMR to obtain spatial distribution information. Spatial information can be obtained by imposing a slight gradient on the static magnetic field. Because the resonance frequency of the signal from the nuclei is proportional to the field, it is possible to derive the position of the nuclei by imposing gradients in different directions. Three-dimensional reconstruction can be performed using algorithms similar to those for x-ray CT.

In vivo Spectroscopy

In addition to proton density and relaxation time distributions, phosphorus chemical state analysis has emerged as an important medical application of NMR. Imaging of phosphorus is not currently feasible because of its low concentration. However, NMR spectroscopy can be used in vivo to measure intracellular *p*H and the relative concentrations of phosphocreatine, ATP, and inorganic phosphate in intact animals and humans for the investigation of oxidative phosphorylation processes in large tissue volumes. Human limbs, living animals, beating hearts, and other organs or tissues have been immersed in high-field magnets for NMR spectroscopy in studies of energy metabolism (*72, 73*). Tissue *p*H can be inferred from the positions of inorganic phosphorus peaks. By using an RF coil placed near the surface of the body to obtain a spectrum from the region near the coil, it is possible to acquire data that reflect the changes in the energy state of phosphorus in brain, the body periphery, and potentially the heart. Another approach, which involves shaping a region of locally uniform magnetic field to sample a large but known volume in the body, has also been adapted to phosphorus spectroscopy for tissues within the body (*74*).

One reason why phosphorus NMR measurements require different methods than those employed for hydrogen is that the phosphorus signals are comparatively weak. The concentrations of phosphorus metabolites in tissues are 10^{-4} times the concentration of hydrogen. Thus phosphorus spectra in humans and large animals are not expected to be observed in volumes smaller than about 10 cm^3. In addition, the higher fields (near 1.5 T) needed to separate the peaks in the spectra sufficiently for analysis result in a

higher resonance frequency. At higher frequencies the depth of penetration of the RF signal is limited, so that distortions similar to the attenuation distortion in single-photon tomography (*5*) will occur if the usual imaging techniques are used. The problem of uniformity over the image plane is avoided by using local detection with shaped fields over large volumes, or coils on the surface of the body. Another interesting use of this local detection technique is to observe the NMR signal when a small electromagnet placed close to the body is suddenly deenergized. A resonance RF signal can be observed in the natural magnetic field of the earth and relaxation times may be measured in vivo for blood, urine, amniotic fluid, and ingested liquids (*75*).

Future Medical Uses of Nuclear Magnetic Resonance

It appears that NMR instrumentation will be developed along two lines: (i) to produce high-resolution hydrogen imaging systems for the head and the body with magnetic fields between 0.1 and 0.5 T, and (ii) to produce high-field instruments (0.4 to 2.0 T) for phosphorus imaging of known, relatively large (1 to 100 cm^3) regions of the body with shaped fields and coils mounted on the body surface. Conventional electromagnets are adequate for low fields; however, above approximately 0.3 T, superconducting magnets are preferred because of the power savings they provide for daily operation and their stability.

In summary, the five physical characteristics that NMR can measure in the human body are: (i) concentrations of nuclei such as hydrogen, carbon, sodium, fluorine, phosphorus, and other elements with appropriate nuclear characteristics; (ii) T_1 relaxation time; (iii) T_2 relaxation time; (iv) chemical shift, which is the small change in the resonance frequency associated with electronically induced magnetic field perturbation due to chemical bonds near the nuclei of interest; and (v) volume flow information related to the change in signal intensity due to movement of magnetized nuclei through the resonance region.

The health hazards from static field effects, induced currents, and RF heating are not believed to be significant with present instrumentation (*76*). The instrumentation required is similar in complexity and cost to that of x-ray CT, and the broad range and flexibility of NMR suggest that it may have profound advantages for medical diagnostic imaging by use of protons and other nuclei for noninvasive measurements of tissue composition (*77, 78*).

Discussion

Over the past 10 years there has been a dramatic evolution in radiological imaging for both clinical diagnosis and noninvasive medical research. In good part this has been the result of the application of digital computers. It has sometimes appeared that various modalities were in competition; however, with further development it has become clear that they measure different specific parameters (Table 1). X-ray CT scanning measures tissue density, PET in vivo biochemistry, and NMR the concentration and molecular state of atoms such as hydrogen and phosphorus. Each will have its special place in medicine.

X-ray CT scanning made spectacular clinical contributions in the first year after its introduction. Such dramatic short-term results have not been obtained with PET, and NMR is just being introduced commercially. Both positron and single-photon emission tomography have already proved clinically valuable in revealing pathologies invisible to the CT scanner. Their applications have so far been largely limited to measurements of blood flow and metabolism in brain and heart. Completely new horizons may be opened up by the realization of PET's theoretical ability to localize neurotransmitter receptors in the brain.

Potential uses of NMR are based on its ability to provide information on the anatomic distribution of hydrogen with diagnostic end points similar to those of x-ray CT and, even more promising, information on the relative locations and concentrations of selected atoms in different chemical states in tissue (*72, 78*). The sensitivity of NMR for studies of chemical elements cannot approach that of PET, yet its ability to distinguish lesions of multiple sclerosis and to provide early diagnosis of ischemic brain disease suggests that it may supplement or even replace x-ray CT in many clinical applications.

The major contribution of PET and NMR might not be to day-to-day clinical diagnosis but rather to investigations of disease processes and natural life processes that heretofore have been inhibited by the lack of noninvasive techniques for in vivo biochemical measurements. Since biological imaging offers the opportunity to investigate the brain and other organs at work in health and disease, the likelihood that it will yield results bearing directly on the diagnosis, prevention, and treatment of disease is high compared with that of alternatives competing for the same financial resources.

References and Notes

1. "Conference on Biological Imaging: Contributions from Contemporary Physics and Engineering," held on 16 to 18 November 1980 at Scripps Clinic and Research Foundation, La Jolla, Calif.
2. H. J. Berger, A. Gottschalk, B. L. Zaret, *Radiol. Clin. North Am.* **18**, 441 (1980).
3. E. L. Ritman, J. H. Kinsey, R. A. Robb, B. K. Gilbert, L. D. Harris, E. H. Wood, *Science* **210**, 273 (1980); D. P. Boyd, R. G. Gould, J. R. Quinn, R. Sparks, J. H. Stanley, W. B. Herrmannsfeldt, *IEEE Trans. Nucl. Sci.* **NS-26**, 2724 (1979).
4. M. P. Capp, *Radiology* **138**, 541 (1981); C. A. Mistretta, A. B. Crummy, C. M. Strother, *ibid.* **139**, 273 (1981); B. J. Hilman *et al.*, *ibid.*, p. 277; C. A. Mistretta and A. B. Crummy, *Science* **214**, 761 (1981).
5. T. F. Budinger, G. T. Gullberg, R. H. Huesman, in *Image Reconstruction from Projections: Implementation and Applications*, G. T. Herman, Ed. (Springer, Berlin, 1979), pp. 147–246; G. T. Gullberg and T. F. Budinger, *IEEE Trans. Biomed. Eng.* **BME-28**, 142 (1981).
6. D. E. Kuhl and R. Q. Edwards, *Radiology* **80**, 653 (1963).
7. H. O. Anger, in *Fundamental Problems in Scanning*, A. Gottschalk and R. N. Beck, Eds. (Thomas, Springfield, Ill., 1968), pp. 195–211.
8. D. E. Kuhl, M. Reivich, A. Alavi, I. Nyary, M. M. Staum, *Circ. Res.* **36**, 610 (1975); D. E. Kuhl *et al.*, *J. Neurosurg.* **52**, 309 (1980).
9. N. A. Lassen, L. Henriksen, O. Paulson, *Stroke* **12**, 284 (1981); F. Bonte and E. Stokely, *J. Nucl. Med.* **22**, 1049 (1981); T. E. Budinger, *ibid.*, p. 1094; D. E. Kuhl, J. L. Wu, T. H. Lin, C. Selin, M. Phelps, *J. Cereb. Blood Flow Metab.* **1** (Suppl. 1), S25 (1981).
10. G. L. Brownell and W. H. Sweet, *Nucleonics* **11**, 40 (1953); H. O. Anger and D. J. Rosenthal, in *Medical Radioisotope Scanning* [International Atomic Energy Agency (IAEA) and World Health Organization, Vienna, 1959], pp. 59–82.
11. L. A. Shepp and B. F. Logan, *IEEE Trans. Nucl. Sci.* **NS-21**, 21 (1974); D. A. Chesler, in *Tomographic Imaging in Nuclear Medicine*, G. S. Freedman, Ed. (Society of Nuclear Medicine, New York, 1973), p. 176.
12. M. E. Phelps, *Semin. Nucl. Med.* **7**, 337 (1977); G. L. Brownell, J. A. Correia, R. Zamenhof, *Recent Adv. Nucl. Med.* **5**, 1 (1979).
13. C. Burnham *et al.*, *IEEE Trans. Nucl. Sci.* **NS-28**, 109 (1981).
14. T. F. Budinger, S. E. Derenzo, G. T. Gullberg, R. H. Huesman, *ibid.* **NS-26**, 2742 (1979).
15. C. A. Burnham, S. Aronow, G. L. Brownell, *Phys. Med. Biol.* **15**, 517 (1970); C. S. Burnham and G. L. Brownell, *IEEE Trans. Nucl. Sci.* **NS-19**, 3 (1972); G. L. Brownell and C. A. Burnham, in *Tomographic Imaging in Nuclear Medicine*, G. S. Freedman, Ed. (Society of Nuclear Medicine, New York, 1973), p. 154.
16. M. M. Ter-Pogossian *et al.*, *Radiology* **114**, 89 (1975); M. D. Phelps, E. J. Hoffman, N. A. Mullani, *J. Nucl. Med.* **16**, 210 (1975).
17. E. J. Hoffman, M. E. Phelps, N. A. Mullani, C. S. Higgins, M. M. Ter-Pogossian, *J. Nucl. Med.* **17**, 493 (1976); M. M. Ter-Pogossian, N. A. Mullani, J. T. Hood, C. S. Higgins, C. M. Currie, *Radiology* **128**, 477 (1978).
18. J. S. Robertson *et al.*, in *Tomographic Imaging in Nuclear Medicine*, G. S. Freedman, Ed. (Society of Nuclear Medicine, New York, 1973), p. 142; C. J. Thompson, Y. L. Yamamoto, E. Mayer, *Proc. Soc. Photo-Opt. Instrum. Eng. 96* (1976); *IEEE Trans. Nucl. Sci.* **NS-26**, 583 (1979).
19. S. E. Derenzo, T. F. Budinger, R. H. Huesman, J. L. Cahoon, T. Vuletich, *IEEE Trans. Nucl. Sci.* **NS-28**, 81 (1981).
20. R. A. Brooks, V. J. Sank, W. S. Friauf, S. B. Leighton, H. E. Cascio, G. Di Chiro, *IEEE Trans. Biomed. Eng.* **BME-28**, 158 (1981); E. Tanaka *et al.*, *IEEE Trans. Nucl. Sci.* **NS-26**, 2728 (1979); L. Eriksson *et al.*, *ibid.* **NS-25**, 624 (1978); I. Kanno, K. Vermura, S. Miura, Y. Miura, *J. Compt. Assist. Tomogr.* **5**, 216 (1981).
21. N. A. Mullani, J. Markham, M. M. Ter-Pogossian, *ibid.* **21**, 1095 (1980); R. Allemand, C. Gresset, J. Vacher, *ibid.*, p. 153; M. M. Ter-Pogossian, N. A. Mullani, D. C. Ficke, *J. Com-*

put. Assist. Tomogr. **5**, 227 (1981); D. L. Snyder, L. J. Thomas, Jr., M. M. Ter-Pogossian, *IEEE Trans. Nucl. Sci.* **NS-28**, 3575 (1981).
22. Z. H. Cho and M. R. Faruki, *J. Nucl. Med.* **18**, 840 (1977); S. E. Derenzo, *ibid.* **21**, 971 (1980); *IEEE Trans. Nucl. Sci.* **NS-28**, 131 (1981).
23. T. F. Budinger, W. L. Greenberg, S. E. Derenzo, G. T. Gullberg, R. H. Huesman, *J. Nucl. Med.* **19**, 309 (1978).
24. A. P. Wolf and C. S. Redvanly, *Int. J. Appl. Radiat. Isot.* **28**, 29 (1977); M. J. Welch and S. Wagner, *Recent Adv. Nucl. Med.* **5**, 51 (1979); J. C. Clark and P. D. Buckingham, *Short-lived Radioactive Gases for Clinical Use* (Butterworths, London, 1975).
25. J. F. Lifton and M. J. Welch, *Radiat. Res.* **45**, 35 (1971).
26. M. M. Ter-Pogossian, J. O. Eichling, D. O. Davis, M. J. Welch, *J. Clin. Invest.* **49**, 381 (1970); ———, J. M. Metzger, *Radiology* **93**, 31 (1969).
27. R. Subramanyam, N. M. Alpert, B. Hoop, G. L. Brownell, J. M. Taveras, *J. Nucl. Med.* **19**, 48 (1978).
28. A. S. Gelbard, C. P. Clarke, J. S. Laughlin, *Radiology* **116**, 127 (1975); *J. Nucl. Med.* **15**, 1223 (1974); M. B. Cohen, *et al.*, in *Radiopharmaceuticals*, G. Subramanyam *et al.*, Eds. (Society of Nuclear Medicine, New York, 1975), p. 184.
29. T. Ido, C. N. Wan, J. S. Fowler, A. P. Wolf, *J. Org. Chem.* **42**, 2341 (1977); B. M. Gallagher *et al.*, *J. Nucl. Med.* **18**, 990 (1977).
30. For extensive coverage of receptor site evaluation and radiopharmaceuticals, see W. Eckelman, Ed., *Receptor Binding Radiotracers* (CRC Press, Boca Raton, Fla., 1982), vol. 1, p. 200; vol. 2, p. 248.
31. D. Comar, M. Maziere, C. Crouzel, *Radiopharmaceuticals and Labelled Compounds* (IAEA, Vienna, 1973), p. 461; D. Comar, M. Maziere, C. Marazano, C. Raynaud, *J. Nucl. Med.* **16**, 521 (1975).
32. D. Comar *et al.*, *Nature (London)* **280**, 329 (1979).
33. Y. L. Yamamoto *et al.*, *J. Comput. Assist. Tomogr.* **1**, 43 (1977).
34. T. Jones, G. L. Brownell, M. M. Ter-Pogossian, *J. Nucl. Med.* **15**, 505 (1974).
35. P. V. Harper, K. A. Lathrop, H. Krizek, N. Lembares, V. Stark, P. B. Hoffer, *ibid.* **13**, 278 (1972); M. E. Phelps *et al.*, *ibid.* **19**, 1311 (1978); H. R. Schelbert *et al.*, *Am. J. Cardiol.* **43**, 209 (1979); K. L. Gould, H. R. Schelbert, M. E. Phelps, E. J. Hoffman, *ibid.*, p. 200.
36. T. F. Budinger, Y. Yano, B. Hoop, Jr., *J. Nucl. Med.* **16**, 429 (1975).
37. G. Lenz, T. Jones, G. G. McKenzie, *J. Neurol. Neurosurg. Psychiatry* **41**, 1 (1978); *ibid.*, p. 11.
38. N. M. Alpert, J. A. Correia, R. H. Ackerman, A. Gouliamos, G. L. Brownell, J. M. Taveras, *J. Nucl. Med.* **19**, 700 (1978).
39. G. L. Brownell and S. Cochavi, *J. Comput. Assist. Tomogr.* **2**, 533 (1978).
40. M. E. Raichle, K. B. Larson, M. E. Phelps, R. L. Grubb, Jr., M. J. Welch, M. M. Ter-Pogossian, *Am. J. Physiol.* **228**, 1936 (1975); M. E. Raichle, M. J. Welch, R. L. Grubb, Jr., C. S. Higgins, M. M. Ter-Pogossian, K. B. Larson, *Science* **199**, 986 (1977).
41. L. Sokoloff *et al.*, *J. Neurochem.* **28**, 897 (1977).
42. M. Reivich *et al.*, *Circ. Res.* **44**, 127 (1979).
43. M. E. Phelps, S. C. Huang, E. J. Hoffman, C. Selin, L. Sokoloff, D. E. Kuhl, *Ann. Neurol.* **6**, 371 (1979); G. L. Brownell, R. H. Ackerman, H. W. Strauss, *J. Comput. Assist. Tomogr.* **4**, 473 (1980); M. E. Phelps *et al.*, *Neurology (N.Y.)* **31**, 517 (1981); P. D. Crane, W. M. Pardridge, L. D. Braun, A. M. Nyerges, W. H. Oldendorf, *J. Neurochem.* **36**, 1601 (1981).
44. D. E. Kuhl, M. E. Phelps, A. P. Kowella, E. J. Metter, C. Selin, J. Winter, *Ann. Neurol.* **8**, 47 (1980).
45. R. H. Ackerman *et al.*, *Arch. Neurol.* **38**, 537 (1981).
46. C.-K. Yen and T. F. Budinger, *J. Comput. Assist. Tomogr.* **5**, 792 (1981).
47. M. E. Phelps, D. E. Kuhl, J. C. Mazziotta, *Science* **211**, 1445 (1981).
48. C. Kennedy *et al.*, *Proc. Natl. Acad. Sci. U.S.A.* **73**, 4230 (1976).
49. D. H. Huben, T. N. Wiesel, M. P. Stryker, *J. Comp. Neurol.* **77**, 361 (1978).
50. E. S. Weiss *et al.*, *Circ. Res.* **39**, 24 (1976); E. J. Hoffman *et al.*, *J. Nucl. Med.* **18**, 57 (1977).
51. H. R. Schelbert, M. E. Phelps, C. Selin, R. C. Marshall, E. J. Hoffman, D. E. Kuhl, in *Advances in Clinical Cardiology: Quantification of Myocardial Ischemia*, H. W. Heiss, Ed. (Witzstrock, New York, 1980), vol. 1, p. 437.
52. E. J. Hoffman *et al.*, *J. Comput. Assist. Tomogr.* **3**, 731 (1979); R. H. Huesman and J. L. Cahoon, *IEEE Trans. Nucl. Sci.* **NS-27**, 474 (1980).
53. D. J. Hnatowich, *J. Nucl. Med.* **16**, 764 (1975); F. Bonte, J. Moore, K. Graham, *ibid.*, p. 132.
54. F. Bonte, R. Parkey, J. Moore, E. Stokley, *Radiology* **110**, 473 (1974).
55. S. A. Gronemeyer, G. L. Brownell, D. R. Elmaleh, C. A. Athanasoulis, *Semin. Nucl. Med.* **10**, 392 (1980); S. M. Larsen, Z. Grunbaum, J. S. Rasey, *Radiology* **134**, 771 (1980).
56. T. R. Ligon, thesis, Oklahoma State University (1967); J. A. Jackson and W. H. Langham, *Rev. Sci. Instrum.* **39**, 510 (1968).
57. R. Damadian, *Science* **171**, 1151 (1971).
58. P. C. Lauterbur, *Bull. Am. Phys. Soc.* **18**, 86 (1972); *Nature (London)* **242**, 190 (1973).
59. R. B. Moon and H. J. Richards, *J. Biol. Chem.* **248**, 7276 (1973).
60. "Nuclear Magnetic Resonance (NMR) Imaging Symposium, Nashville, Tennessee, October 26–27, 1980, Proceedings," *J. Comput. Assist. Tomogr.* **5**, 285 (1981); T. C. Farrar and E. D. Becker, *Pulse and Fourier Transform NMR; Introduction to Theory and Methods* (Academic Press, New York, 1971).
61. L. Crooks *et al.*, *Radiology* **136**, 701 (1980).
62. P. C. Lauterbur, M. H. Mendonça Dias, A. M. Rudin, in *Frontiers of Biological Energetics*, P. O. Dutton, J. S. Leigh, A. Scarpa, Eds. (Academic Press, New York, 1978), p. 752.
63. W. S. Hinshaw, E. R. Andrew, P. A. Bottomley, G. N. Holland, W. S. Moore, B. S. Worthington, *Br. J. Radiol.* **52**, 36 (1979); P. Mansfield, P. G. Morris, R. J. Ordidge, I. L. Pykett, V. Bangert, R. E. Coupland, *Philos. Trans. R. Soc. London Ser.* B **289**, 503 (1980).
64. R. C. Hawkes, G. N. Holland, W. S. Moore, B. S. Worthington, *J. Comput. Assist. Tomogr.* **4**, 577 (1980).
65. G. Suryan, *Proc. Indian Acad. Sci. Sect. A* **33**, 107 (1951); J. R. Singer, *Science* **130**, 1652 (1959); in *Nuclear Magnetic Resonance Imaging in Medicine*, L. Kaufman, L. E. Crooks, A. Margulis, Eds. (Ikagu-Shoin, New York, 1981), pp. 128–144; J. H. Battocletti *et al.*, *Med. Phys.* **8**, 435 (1981).
66. W. A. Edelstein, J. M. S. Hutchison, G. Johnson, T. Redpath, *Phys. Med. Biol.* **25**, 751 (1980).
67. W. S. Hinshaw, *Phys. Lett. A* **48**, 87 (1974).
68. R. Damadian, *Philos. Trans. R. Soc. London Ser. B* **289**, 489 (1980); ———, L. Minkoff, M. Goldsmith, J. A. Koutcher, *Naturwissenschaften* **65**, 250 (1978).
69. P. C. Lauterbur and C.-M. Lai, *IEEE Trans. Nucl. Sci.* **NS-27**, 1227 (1980); L. A. Shepp, *J. Comput. Assist. Tomogr.* **4**, 94 (1980); R. B. Marr, C.-N. Chen, P. C. Lauterbur, in *Lecture Notes in Medical Informatics*, vol. 8, *Mathematical Aspects of Computerized Tomography*, G. T. Herman and F. Natterer, Eds. (Springer, Berlin, 1980), pp. 225–240.
70. G. N. Holland, R. C. Hawkes, W. S. Moore, *J. Comput. Assist. Tomogr.* **4**, 429 (1980).
71. For examples, see P. T. Beall, C. F. Hazlewood, P. N. Rao, *Science* **192**, 904 (1976); S. R. Kasturi, S. S. Ranade, S. S. Shaw, *Proc. Indian Acad. Sci. Sect. B* **81**, 60 (1976); R. G. Fruchter, M. Goldsmith, J. G. Boyce, A. D. Nicastri, J. Koutcher, R. Damadian, *Gynecol. Oncol.* **6**, 243 (1978); I. D. Kuntz and A. Zipp, *N. Engl. J. Med.* **297**, 262 (1977); B. M. Fung, *Biochim. Biophys. Acta* **497**, 371 (1977); R. Mathur-De Vré, *Prog. Biophys. Mol. Biol.* **35**, 103 (1979). For sharply critical views, see H. M. Swartz, *J. Magn. Reson.* **29**, 393 (1978); D. P. Hollis, *Bull. Magn. Reson.* **1**, 27 (1979).
72. D. I. Hoult, S. J. W. Busby, D. G. Gadian, G. K. Radda, R. E. Richards, P. J. Seely, *Nature (London)* **252**, 285 (1974); B. Chance, Y. Nakase, M. Bond, J. S. Leigh, Jr., G. McDonald, *Proc. Natl. Acad. Sci. U.S.A.* **75**, 4925 (1978); D. P. Hollis *et al.*, *J. Magn. Reson.* **29**, 319 (1978); G. K. Radda and P. J. A. Seeley, *Rev. Physiol.* **41**, 749 (1979); J. J. H. Ackerman, T. H. Grove, G. G. Wong, D. G. Gadian, G. K. Radda, *Nature (London)* **283**, 167 (1980); M. R. Goldman, G. M. Pohost, J. S. Ingwall, E. T. Fosel, *Am. J. Cardiol.* **46**, 1278 (1980); R. L. Nunnally and P. A. Bottomley, *Science* **211**, 177 (1981).
73. D. G. Gadian and G. K. Radda, *Annu. Rev. Biochem.* **50**, 69 (1981).
74. R. E. Gordon *et al.*, *Nature (London)* **287**, 736 (1980).
75. B. Borcard, E. Hiltbrand, P. Magnin, G. J. Bene, *C. R. Acad. Sci. Ser. B* **288**, 41 (1979).
76. T. F. Budinger, *J. Comput. Assist. Tomogr.* **5**, 800 (1981).
77. F. W. Smith, J. R. Mallard, A. Reid, J. M. S. Hutchison, *Lancet* **1981-I**, 963 (1981); B. D. Ross, G. K. Radda, D. G. Gadian, G. Rocker, M. Esiri, J. Falconer-Smith, *N. Engl. J. Med.* **304**, 1338 (1981); R. C. Hawkes, G. N. Holland, W. S. Moore, E. J. Roebuck, B. S. Worthington, *J. Comput. Assist. Tomogr.* **5**, 605 (1981); *ibid.*, p. 613; F. H. Doyle *et al.*, *Lancet* **1981-II**, 53 (1981); I. R. Young, A. S. Hall, C. A. Pallis, G. M. Bydder, N. J. Legg, R. E. Steiner, *ibid.*, p. 1063.
78. J. L. DeLayre, J. S. Ingwall, C. Malloy, E. T. Fossel, *Science* **212**, 935 (1981); D. M. Kramer, in *Nuclear Magnetic Resonance Imaging in Medicine*, L. Kaufman, L. E. Crooks, A. R. Margulis, Eds. (Igaku-Shoin, New York, 1981), pp. 184–203; J. R. Alger, L. O. Sillerud, K. L. Behar, R. J. Gillies, R. G. Shulman, R. E. Gordon, D. Shaw, P. E. Hanley, *Science* **214**, 660 (1981).
79. We thank C. Green, A. Suttle, and C. C. Edwards for making this analysis possible, and B. Matheson, L. Lutgens, and M. Graham for editorial assistance. This work was supported by the Office of Energy Research, Office of Health and Environmental Research, U.S. Department of Energy, under contract W-7405-ENG-48 and by the National Heart, Lung, and Blood Institute under grant No. PO1 HL25840-01.